

Cerebral muscarinic acetylcholinergic receptor measurement in Alzheimer's disease patients on ^{11}C -N-methyl-4-piperidyl benzilate —Comparison with cerebral blood flow and cerebral glucose metabolism—

Tsuyoshi YOSHIDA,* Yasuo KUWABARA,* Yuichi ICHIYA,* Masayuki SASAKI,* Toshimitsu FUKUMURA,*
Atsushi ICHIMIYA,** Masashi TAKITA,** Koji OGOMORI** and Kouji MASUDA*

*Department of Radiology and **Department of Neuropsychiatry, Faculty of Medicine, Kyushu University

We studied the cerebral muscarinic acetylcholinergic receptor (mACh-R) by means of ^{11}C -N-methyl-4-piperidyl benzilate (^{11}C -NMPB) and positron emission tomography (PET) in Alzheimer's disease (AD) cases, and the findings were compared with the cerebral blood flow (CBF) and the glucose metabolism (CMRGlc) to evaluate the relationship between the mACh-R and the CBF or the CMRGlc. The subjects consisted of 18 patients with AD and 18 age and sex matched normal volunteers. The patients were clinically diagnosed according to the criteria of the NINDS-ADRDA as having "probable AD" and were thus classified into two groups (mild and moderate AD) according to the severity of dementia determined by DSM-III-R. The CBF was measured by $^{99\text{m}}\text{Tc}$ -HMPAO SPECT, and the CMRGlc was measured by ^{18}F FDG PET. The ^{11}C -NMPB uptake was evaluated by the graphical method and the ratio method (ROIs/Cerebellum). A significant mACh-R decrease and more severe CMRGlc decrease in the cortical region was seen in mild and moderate AD. The decrease in the CBF was not as obvious as that in the mACh-R and the CMRGlc.

Our study thus suggested that the mACh-R decreased in patients with AD, and that the ^{18}F FDG PET was the most sensitive method for detecting the degenerative regions in patients with AD.

Key words: cerebral muscarinic acetylcholinergic receptor, ^{11}C -N-methyl-4-piperidyl benzilate, cerebral blood flow, glucose metabolism, Alzheimer's disease

INTRODUCTION

THE "CHOLINERGIC HYPOTHESIS of geriatric memory dysfunction" was first presented by Bartus in 1982¹ and Coyle later extended the cholinergic hypothesis to Alzheimer's disease (AD).² There have been several reports on cerebral muscarinic acetylcholinergic receptor (mACh-R) in AD patients, but the results are still controversial. Mash et al.³ reported a decrease in the cerebral mACh-R by using ^3H -oxotremorine-M in AD patients, and postmortem studies with ^3H -QNB did not show any substantial changes. The *in vivo* study of the mACh-R in AD with ^{123}I -QNB and single-photon emis-

sion tomography (SPECT) revealed a significant decrease in the temporal and parietal cortices,⁴ but a PET study revealed no decrease in the mACh-R binding in AD with ^{11}C -tropanyl benzilate (TRB).⁵

^{11}C -NMPB is a ligand which shows a greater brain uptake and higher affinity for the mACh-R in the brain.⁶ This ligand was first synthesized for a PET study by Mulholland et al.,⁷ and high uptake into the human cortices and basal ganglia was confirmed by Koeppe et al.,⁸ but preliminary results with ^{11}C -NMPB by Zubieta et al. failed to demonstrate any decrease in the mACh-R binding in AD.⁹ In the present study, the mACh-R in AD patients was evaluated with ^{11}C -NMPB, and then the findings were compared with the cerebral blood flow (CBF) and the glucose metabolism (CMRGlc) to evaluate the relationship between them. And we also estimated the relationship between the ^{11}C -NMPB uptake and mental function in AD patients.

Received June 11, 1997, revision accepted December 1, 1997.

For reprint contact: Tsuyoshi Yoshida, M.D., Department of Radiology, Kyushu University, 3-1-1 Maidashi, Higashi-ku, Fukuoka 812-8582, JAPAN.

Table 1 Patient characteristics and clinical data

No.	Age/Sex	Severity of dementia (DSM-III-R)	Intelligence test					Duration from disease onset (years)	Cerebral imaging CT/MRI	
			HDRS	MMSE	WAIS-R				atrophy	WML
					V-IQ	P-IQ	T-IQ			
1	59/M	mild	26	26	149	111	134	2	mild	mild
2	60/F	mild	20	20		n.d.		0.5	moderate	—
3	64/F	mild	15	23	95	105	100	1.5	mild	—
4	67/F	mild	7	14	67	60	62	7	mild	mild
5	71/F	mild	26	20	100	97	98	3	mild	—
6	74/F	mild	21	20	90	90	92	1	mild	mild
7	75/F	mild	n.d.	14	81	75	76	1	mild	mild
8	53/M	moderate	22	18	66	55	57	1	—	—
9	57/F	moderate	15	13	62	50	55	0.5	mild	—
10	60/M	moderate	n.d.	9		n.d.		0.5	mild	mild
11	60/M	moderate	15	20	74	87	79	2	moderate	—
12	61/F	moderate	14	12		n.d.		3	mild	—
13	62/F	moderate	3	6	49	0	42	2	moderate	mild
14	65/F	moderate	19	23	113	96	105	3	mild	mild
15	65/F	moderate	22	21	92	80	85	3	mild	mild
16	68/M	moderate	6	14	55	52	51	0.5	moderate	mild
17	69/M	moderate	23	23	102	100	101	1	mild	—
18	80/F	moderate	11	8		n.d.		4	moderate	mild

DSM-III-R: Diagnostic and statistical manual of mental disorders, third edition, revised, mod.: moderate, HDRS: Hasegawa dementia rating scale, MMSE: mini-mental state examination, WAIS-R: Wechsler adult intelligence scale, revised, T-IQ: Total intelligence quotient, V-IQ: Verbal IQ, P-IQ: Performance IQ, WML: white matter lesion(s), n.d.: study not done, —: Negative

SUBJECTS AND METHODS

The subjects consisted of 18 patients with AD and 18 age and sex matched volunteers who were social workers. The patients with AD were clinically diagnosed according to the criteria of the National Institute for Neurological Diseases and Stroke/Alzheimer's Disease and Related Disorders Association (NINDS-ADRDA) for the diagnosis of "probable Alzheimer's Disease."¹⁰ Any patients with infarcts or multiple white matter lesions on MRI or CT were excluded. The patients were classified into two groups, the mildly demented group (mild AD) and moderately demented group (moderate AD), according to the severity of dementia based on the Diagnostic and Statistical manual of Mental disorders, third edition, revised (DSM-III-R).¹¹ The intellectual function was also evaluated with the mini-mental state examination (MMSE),¹² the Hasegawa Dementia Rating Scale (HDRS)¹³ and the Wechsler Adult Intelligence Scale, revised (WAIS-R) (Table 1).

The volunteers were selected after undergoing intelligence tests, brain imaging such as CT and MRI and chemical blood examinations.

¹¹C-NMPB was synthesized by *N*-methylation of 4-piperidyl benzilate with ¹¹C-methyl iodide according to the method of Suhara et al.¹⁴ Radiochemical purity was 98% and specific activity was from 3.89 to 4.61 GBq/ μ mol. ¹⁸F-DG was synthesized by the method reported by Bida et al.¹⁵ Radiochemical purity was 95% and specific

activity was 200 ± 50 GBq/ μ mol. The radiochemical purity of the ^{99m}Tc-HMPAO (Ceretek®, Amersham Ltd., Amersham, UK) was 90%.

PET studies were performed with a PET system HEADTOME-III (Shimadzu Corp., Kyoto, Japan) with a spatial resolution of 8.2 mm full width at half maximum (FWHM) which can simultaneously obtain 5 contiguous slices. A transmission scan with a ⁶⁸Ge/⁶⁸Ga ring source was obtained previous to the emission scans for the correction of attenuation. The ¹¹C-NMPB PET data were obtained every 2 min for 20 min, every 4 min for next 40 min, and at 70 and 90 min (the sampling time was 15 minutes) after the intravenous slow administration of 185 to 1,277 MBq of ¹¹C-NMPB at levels of +2 cm, +3.5 cm, +5 cm, +6.5 cm and +8 cm above the orbitomeatal (OM) line. The CBF was evaluated by ^{99m}Tc-HMPAO SPECT. ^{99m}Tc-HMPAO SPECT studies were performed with a three headed SPECT system GCA 9300A/HG (Toshiba, Tokyo, Japan), equipped with a fan beam collimator (64 × 64 matrix) which provides a spatial resolution of 7.4 mm FWHM. Each detector continuously rotated 120 degrees every 3 minutes in a clockwise and counterclockwise direction for a total of 15 minutes. The axial slice distance was 7.4 mm. The ^{99m}Tc-HMPAO SPECT data were obtained from 15 to 30 min after the intravenous bolus administration of 740 MBq of ^{99m}Tc-HMPAO. The ^{99m}Tc-HMPAO image was reconstructed with a Butterworth filter (cutoff 0.24 cycle/cm and order 8) and ramp filter, and attenuation correction was done by the Chang method¹⁶

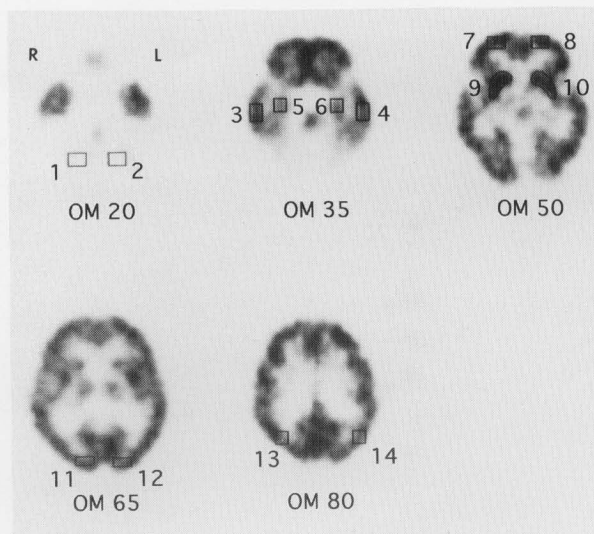


Fig. 1 Regions of interest (ROIs) in the ^{11}C -NMPB uptake images of a 70-year-old male normal volunteer. 1,2: cerebellum, 3,4: temporal cortex, 5,6: hippocampus, 7,8: frontal cortex, 9,10: striatum, 11,12: occipital cortex, 13,14: parietal cortex

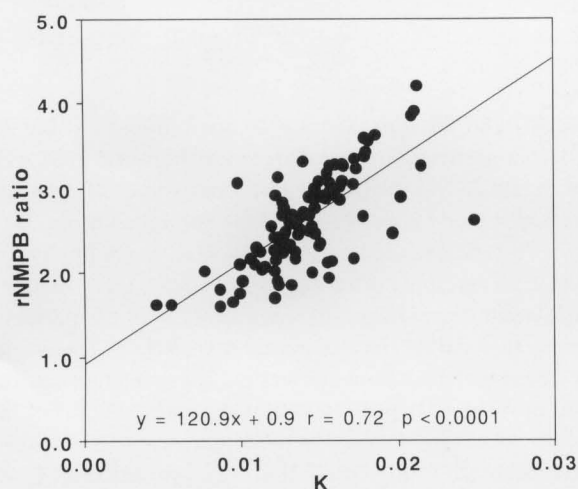


Fig. 2 Correlation between the K value, which reflecting net binding rate to mACh-R in this study, and the regional ^{11}C -NMPB uptake ratio (rNMPB ratio) in the 6 cerebral regions of 8 volunteers and 8 patients with AD. A positive correlation between the K and the rNMPB ratio was shown.

with an attenuation coefficient of 0.12 cm^{-1} . A linearization correction of Lassen et al.¹⁷ was also performed (α constant of 1.51 and Fr of 55 ml/min was employed: α is a correction factor for the linearization¹⁷ and Fr represents cerebellar blood flow) because the $^{99\text{m}}\text{Tc}$ -HMPAO SPECT underestimates the CBF in the high flow region due to accelerated back diffusion. And then the rCBF ratio (cerebral blood flow in an interested region/cerebellar blood flow) was obtained.

The CMRGlc was measured by the ^{18}F FDG method. The PET scan was started 63 min after the intravenous slow

administration of 182 to 377 MBq of ^{18}F FDG. The PET data were obtained for 16 min (8 min/frame) at 10 contiguous slices (OM line +2 cm, +2.7 cm, +3.5 cm, +4.2 cm, +5 cm, +5.7 cm, +6.5 cm, +7.2 cm, +8 cm and +8.7 cm, respectively). Arterial blood was drawn every 15 sec for 2 min, every 30 sec for 2 min, every 1 or 2 min for 4 min, every 4 min for 12 min and every 10 min for 50 min. The regional CMRGlc (rCMRGlc) was calculated with the model of Phelps et al.,¹⁸ later modified by Brooks.¹⁹ No significant difference in the serum glucose concentration was observed among the normal controls ($101.4 \pm 6.4\text{ mg/dl}$; mean \pm SD) and patients with mild (106.8 ± 6.4) or moderate AD (108.4 ± 14.7). Each study was performed within 2 weeks in 17 cases, within 1 month in 10 cases, and within 3 months in 9 cases. No significant difference between the patients with mild and moderate AD was seen in the MMSE.

The regions of interest (ROIs) were first established basis of the ^{11}C -NMPB images (the cerebellum ($14 \times 18\text{ mm}$), the frontal, the temporal, the parietal ($14 \times 18\text{ mm}$) and the occipital ($10 \times 18\text{ mm}$) cortices, the hippocampus ($14 \times 14\text{ mm}$) and the striatum (multiangular shape)) (Fig. 1). We rotated and moved the images of ^{18}F FDG to coincide with those of ^{11}C -NMPB. The ROIs on $^{99\text{m}}\text{Tc}$ -HMPAO images were separately drawn while referring to the ROIs on ^{11}C -NMPB images, because the $^{99\text{m}}\text{Tc}$ -HMPAO image slice was thinner than that of the ^{11}C -NMPB images. The mean values in the ROIs on both sides were averaged into a single value and compared in the age-matched normal controls and the patients with AD.

We first used the graphical method of Gjedde and Patlak^{20,21} modified by Suhara et al.¹⁴ and then used the ratio method²² for a ^{11}C -NMPB analysis. In the former method, Suhara et al. used the cerebellar radioactivities as an input function instead of the sequential arterial blood plasma activities.¹⁴ With their method, we plotted the ratio of radioactivity in a region of interest to that in the cerebellum versus the normalized integral of radioactivity in the cerebellum. Between 40 and 120 min of the normalized integral, the plotted points yielded a straight line by the least squares fitting and the slope of the line (K value), which has been thought to be net binding rate including the association rate constant of the ligand with the receptors¹⁴ and the possible effects of the ligand transport rate ($\text{CBF} \times \text{First pass extraction fraction}$).⁹ In the latter method, we used the ratio of radioactivity (regional ^{11}C -NMPB uptake ratio (rNMPB ratio)) for 15 min (from 85 to 100 min) after injection.

We calculated the K and the rNMPB ratio in the 6 cerebral regions of 8 volunteers and 8 patients with AD (total 96 regions) and evaluated the correlation between the two parameters by means of a single regression analysis. A positive correlation was then seen between the K and the rNMPB ratio ($Y = 120.9X + 0.9$, $r = 0.72$, $p < 0.0001$; Fig. 2). Thus we use the rNMPB ratio for a ^{11}C -NMPB analysis instead of the K value. Then we compared

Table 2 Comparisons between normal controls and patients with Alzheimer's disease in the rNMPB ratio#, the rCBF ratio## and the rCMRGlc

Study	Location	Normal controls (mean \pm SD)	mild AD (mean \pm SD)	moderate AD (mean \pm SD)
rNMPB ratio	Frontal cortex	n = 18 2.68 \pm 0.32	n = 7 2.41 \pm 0.30	n = 11 2.26 \pm 0.50*
	Temporal cortex	2.68 \pm 0.33	2.35 \pm 0.25	2.27 \pm 0.42*
	Parietal cortex	2.85 \pm 0.40	2.34 \pm 0.31*	2.25 \pm 0.50**
	Occipital cortex	3.07 \pm 0.42	2.75 \pm 0.22	2.64 \pm 0.39*
	Hippocampus	2.29 \pm 0.31	1.97 \pm 0.30	1.88 \pm 0.27**
	Striatum	3.10 \pm 0.39	3.03 \pm 0.28	2.81 \pm 0.57
rCBF ratio	Frontal cortex	n = 18 0.81 \pm 0.10	n = 7 0.75 \pm 0.09	n = 11 0.72 \pm 0.09
	Temporal cortex	0.78 \pm 0.06	0.71 \pm 0.08	0.72 \pm 0.07
	Parietal cortex	0.82 \pm 0.09	0.71 \pm 0.12	0.70 \pm 0.13*
	Occipital cortex	0.78 \pm 0.13	0.78 \pm 0.10	0.76 \pm 0.10
	Hippocampus	0.71 \pm 0.07	0.60 \pm 0.04**	0.66 \pm 0.08
	Striatum	0.92 \pm 0.12	0.88 \pm 0.10	0.95 \pm 0.11
rCMRGlc	Frontal cortex	n = 13 7.67 \pm 0.69	n = 6 6.59 \pm 0.71*	n = 7 5.83 \pm 1.11***
	Temporal cortex	7.45 \pm 0.73	6.07 \pm 0.78*	5.78 \pm 1.27**
	Parietal cortex	7.90 \pm 0.89	6.15 \pm 1.16*	6.09 \pm 1.90*
	Occipital cortex	7.97 \pm 0.92	6.91 \pm 0.75	6.99 \pm 1.24
	Hippocampus	5.82 \pm 0.79	4.80 \pm 0.55*	4.78 \pm 0.39**
	Striatum	8.29 \pm 0.68	7.31 \pm 0.94	7.04 \pm 0.90*

#: Cerebral ^{11}C -NMPB radioactivity in the region of interest/Cerebellar radioactivity

##: Cerebral blood flow in the region of interest/Cerebellar blood flow

AD: Alzheimer's disease, Significant decrease between the normal controls and AD, *: $p < 0.05$, **: $p < 0.01$, ***: $p < 0.001$

the rNMPB ratio, the rCBF ratio and the rCMRGlc by using the AD/NC ratio (the mean value for the patients with AD/the mean value of the normal controls).

This study was approved by the committee for the clinical application of cyclotron-producing radionuclides in Kyushu University Hospital, and informed consent was obtained from all normal volunteers, patients and/or their families before the PET and SPECT study.

STATISTICS

Statistical analyses were performed according to the following methods. The comparisons of the rNMPB ratio, the rCBF ratio and the rCMRGlc among the normal controls and the two groups of patients with AD were done by One-way Factorial Analysis of Variance (ANOVA) and multiple comparison tests and Scheffe's method as a Post-Hoc test.²³ Correlations between the rNMPB ratio, the rCBF ratio, the rCMRGlc and the MMSE (or HDRS) were evaluated by Spearman rank correlation and multiple comparison tests (Bonferroni).²⁴ The correlations and differences in comparisons were assessed at a significance threshold of $p < 0.05$.

RESULTS

1. The rNMPB ratio, the rCBF ratio and the rCMRGlc in the patients with AD

The rNMPB ratio, the rCBF ratio and the rCMRGlc in each cerebral region in the patients with mild and moder-

ate AD and the normal controls are shown in Table 2. There were no significant differences between mild and moderate AD in the three values, but some differences were observed between AD and the normal controls. The rNMPB ratio revealed a significant decrease in moderate AD in all cerebral cortices ($p < 0.05$ – 0.001), but in mild AD, a significant decrease was seen only in the parietal cortex ($p < 0.05$). The rCBF ratio revealed no significant decrease in the cerebral cortices except in the hippocampus in mild AD ($p < 0.05$) and the parietal cortex in moderate AD ($p < 0.05$). The rCMRGlc revealed a significant decrease in the cerebral cortices in mild AD ($p < 0.05$). In moderate AD, a much more severe decrease in rCMRGlc was observed ($p < 0.05$ – 0.001).

In the rCBF ratio, the decrease in the AD/NC ratio in mild AD was as much as that in moderate AD, but both in the rNMPB ratio and in the rCMRGlc a larger decrease in the AD/NC ratio was seen in cases of moderate AD than in those with mild AD. In mild AD, the decrease in the AD/NC ratio in the rNMPB ratio was close to that in the rCBF ratio rather than that in the rCMRGlc. In moderate AD, the decrease in the AD/NC ratio in rNMPB ratio was more similar to that in the rCMRGlc than that in the rCBF ratio.

2. Correlation between the rNMPB ratio, the rCBF ratio, the rCMRGlc and the MMSE (or HDRS)

We calculated the ρ (coefficient of Spearman rank correlation) and p -value for the rNMPB ratio, the rCBF ratio, the rCMRGlc and the MMSE in each cerebral region

Table 3 Spearman rank correlations between the rNMPB ratio#, the rCBF ratio##, the rCMRGlc, and the MMSE in Alzheimer's disease

Location	rNMPB ratio (n = 18, m : f = 6 : 12)	rCBF ratio (n = 18, m : f = 6 : 12)	rCMRGlc (n = 13, m : f = 5 : 8)
	ρ	ρ	ρ
Frontal cortex	0.32	0.23	0.72*
Temporal cortex	0.67**	0.58*	0.70*
Parietal cortex	0.68**	0.32	0.61*
Occipital cortex	0.37	- 0.12	0.53
Hippocampus	0.26	- 0.03	0.58*
Striatum	0.32	- 0.07	0.78**

#: Cerebral ^{11}C -NMPB radioactivity in the region of interest/Cerebellar radioactivity

##: Cerebral blood flow in the region of interest/Cerebellar blood flow

ρ : coefficient of Spearman rank correlation, *: $p < 0.05$, **: $p < 0.01$

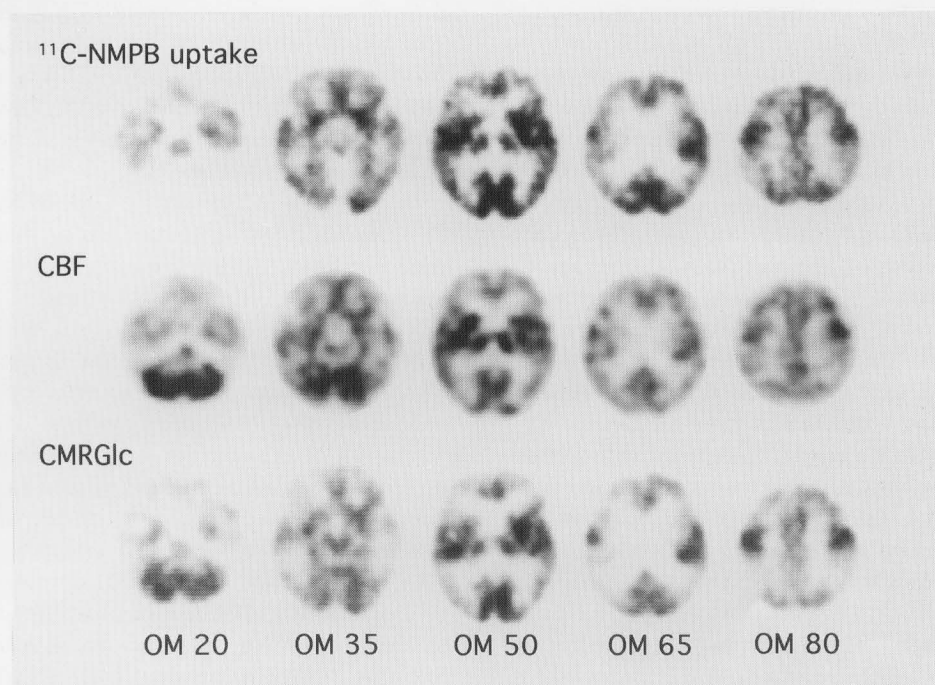


Fig. 3 The ^{11}C -NMPB uptake (upper rows), CBF (middle rows) and CMRGlc (lower rows) images of a 60-year-old patient with moderate Alzheimer's disease. A decrease in the ^{11}C -NMPB uptake and the CBF was observed in the frontal, temporal and parietal cortices while a much larger decrease in the CMRGlc is also seen in the same regions.

(Table 3). A positive correlation between the rNMPB ratio and the MMSE was observed in the temporal ($\rho = 0.67$) and the parietal cortices ($\rho = 0.68$). A positive correlation between the rCMRGlc and the MMSE was also observed in the frontal ($\rho = 0.72$) and temporal cortex ($\rho = 0.70$), the hippocampus ($\rho = 0.58$) and the striatum ($\rho = 0.78$). A positive correlation between the rCBF ratio and the MMSE was observed only in the temporal cortex ($\rho = 0.58$). We also calculated the ρ and p -value for the afore-said three parameters and the HDRS in each cerebral region. A positive correlation between the rNMPB ratio and the HDRS was observed in the temporal ($\rho = 0.57$) and the parietal cortices ($\rho = 0.56$). A positive correlation

between the rCMRGlc and the HDRS was also observed in the frontal cortex ($\rho = 0.74$) and the temporal cortex ($\rho = 0.64$). A positive correlation between the rCBF ratio and the HDRS was observed only in the temporal cortex ($\rho = 0.63$).

A significant difference was not observed among the three parameters because of the small number of subjects.

3. Typical images of moderate AD

A 60-year-old male patient is shown in Fig. 3. His MMSE was 9. He had experienced memory disturbance for 5 months and the illness had progressed substantially over the previous two months.

DISCUSSION

1. *mACh-R changes in patients with AD*

Postmortem studies of cerebral mACh-R in AD with ^3H -QNB revealed no substantial overall changes compared to the normal controls.²⁵ In the human *in vivo* mACh-R studies of patients with AD by means of ^{123}I -QNB and SPECT,^{4,26,27} a significant decrease in ^{123}I -QNB uptake was observed in the temporal and parietal cortices, but a human PET study with ^{11}C -TRB⁵ and ^{11}C -NMPB⁹ revealed no loss of the mACh-Rs in patients with AD. On the other hand, our study revealed a decrease in ^{11}C -NMPB uptake in AD. There are several possible reasons for the discrepancies between the three studies.

A previous *in vitro* study suggested that preferential losses of cortical M2 muscarinic receptors occurred in AD.²⁸ Both ^{11}C -NMPB and ^{11}C -TRB do not appear to be specific for either the M1 or M2 muscarinic subtypes.²⁹ The difference between ^{11}C -NMPB and ^{11}C -TRB in the ratio of M1/M2 binding rates may therefore be attributed to the discrepancies in the accumulation of ligands. Comparison of the two ligands in monkey studies suggests that ^{11}C -NMPB interacts more rapidly with the receptors and has a smaller apparent volume of distribution than ^{11}C -TRB. This means that ^{11}C -NMPB may have better sensitivity to the number of receptors in areas of highest concentration (cerebral cortex and striatum).³⁰ The difference in the sensitivity to the number of receptors may also be attributed to the discrepancies.

Zubieta et al. recently reported a decrease in the ligand transport rate and no decrease in the binding potential in patients with AD by using ^{11}C -NMPB and PET, and thus concluded that previous reports of focal reduction in mACh-R ligand distribution were caused by alterations in the radiotracer transport and not in the receptor binding.⁹ In our study, we used the rNMPB ratio as an index of the net binding rate. A decrease in the rNMPB ratio is attributed to decreased mACh-R or decreased radiotracer transport or both, but the discrepancy between the rNMPB ratio and the rCBF ratio is much clearer in moderate AD than in mild AD, so that the change in the rNMPB ratio may mean not only a change in the radiotracer transport but also a change in mACh-R. Asahina et al. also reported a discrepancy between the K and the CBF in their ^{11}C -NMPB study of patients with Parkinson's disease, or an increase in K despite a decrease or lack of change in CBF.³¹

2. *Comparative studies of mACh-R, CMRGlc and CBF in patients with AD*

Zubieta et al. also reported no mACh-R decrease in the hypometabolic cortical region in AD, but our results revealed a significant mACh-R decrease in the cortical region in mild and moderate AD. The discrepancies between Zubieta's results and ours may partly be due to the difference in the severity of the patients' symptoms. In

moderate AD in our study, a large decrease in the rNMPB ratio and the rCMRGlc was seen in cerebral cortices. Assuming that cholinergic cell loss exists in these regions, we can interpret these outcome well. Even in mild AD, a reduced glucose utilization was found to be related to the neuronal dysfunction originating in synaptic damage (which may include a decrease in the mACh-R), because in mild AD, glycolytic metabolism (which mostly occurs in dendrites or axons) shifts to an oxidative metabolism (which is localized to the mitochondria).³² Fukuyama's study also revealed a decrease in rCBF in the hypometabolic region in AD. In our study, the decrease in the rCBF ratio and rCMRGlc in mild AD is larger than those in moderate AD in the hippocampus. These unexpected results may be due to the fact that some patients with mild AD were diagnosed when they experienced only memory disturbance, because the most characteristic and earliest clinical manifestation in patients with AD is a disturbance of memory³³ and hippocampal hypoperfusion and hypometabolism are noted in patients with memory disturbance.³⁴

In a previous study with ^{123}I -QNB SPECT and ^{18}F FDG PET, mACh-R showed larger defects than glucose metabolism in demented patients.²⁶ And comparative studies of ^{123}I -QNB and ^{123}I IMP,⁴ and of ^{123}I -QNB and $^{99\text{m}}\text{Tc}$ -HMPAO²⁷ in AD revealed a relatively preserved mACh-R despite the CBF decrease. In our study, ^{18}F FDG PET was the most sensitive method for detecting the degenerative regions among the three parameters. The discrepancies between earlier comparative studies and our findings are considered to be due to the difference in the severity and pathological stage of the subjects, as well as due to the differences in the ligands (^{11}C -NMPB and ^{123}I -QNB) and the instruments (PET and SPECT). Our results were not considered to show any difference in spatial resolution because the spatial resolution of our SPECT (7.4 mm) is superior to that of PET (8.2 mm) in FWHM.

3. *The relationship between mACh-R, CMRGlc, CBF and mental function in AD patients*

We evaluated the correlation between the rNMPB ratio, the rCBF ratio, the rCMRGlc and the MMSE (or HDRS) in AD. The MMSE (or HDRS) was employed to evaluate the cognitive aspects of mental function. The rCMRGlc was associated with the MMSE in most cerebral regions, and was associated with the HDRS in the frontal and temporal region. Alavi et al. reported a significantly high correlation between the whole cerebral CMRGlc and the MMSE in AD ($\rho = 0.60$, $p < 0.01$).³⁵ There was also a correlation between the rCBF ratio and the MMSE and HDRS in the temporal region in our study, and some previous reports also support our results.³⁶⁻³⁸ The rNMPB ratio was associated with the MMSE (or HDRS) in the temporal and parietal regions. Although no significant difference was observed among the three parameters

because of the small number of subjects, the rCMRGlc showed a close correlation with intellectual function. This may confirm that ^{18}F FDG PET was the most sensitive method for detecting the degenerative regions in AD.

4. The analytical methods in mACh-R measurement

We first used the Graphical method^{14,20,21} and then used the ratio method²² to analyze the ^{11}C -NMPB uptake. The Graphical method can be used to measure the net accumulation of tracer when the dissociation constant is assumed to be negligible. The K value provided by this method is proportional to the receptor binding rate, assuming that the distribution volume of free ligand is constant.³⁹ We used the cerebellar radioactivities instead of the plasma input function, because the cerebellum contains few muscarinic cholinergic receptors⁴⁰ and the cerebellar radioactivities mainly represent the plasma radioactivities if the non-specific binding is negligible. The ratio method never needs either a kinetic analysis or a dynamic scan, and therefore seems appropriate for demented patients who cannot keep still. We used PET data scanning from 85 to 100 min after injection, because the CBF mediates receptor binding in soon after injection, and because the intersubject deviations increase after that time for the insufficient radioactivities. The ^{11}C -NMPB doses administered were between 6 and 127 μg and no correlation was seen between the injected mass and the cerebral ^{11}C -NMPB uptake. The percent injected dose (decay corrected) in the whole brain at 90 min postinjection averaged 2.8% (range 1.1–4.0%) across 11 volunteers while assuming a cerebral volume of 1,200 ml. The average cerebral concentration of ^{11}C -NMPB ranged from 0.5 to 6.1 nmol and it was below the *in vivo* estimates of the mACh-R concentration (not saturated) with ^{11}C -TRB.⁴¹ We therefore used the rNMPB ratio to evaluate mACh-R.

In the neuroreceptor imaging, the CBF delivered ligand into brain tissue through the blood-brain barrier and thereby affected ligand-receptor binding. It is therefore necessary to determine the ligand kinetics *in vivo* to accurately evaluate receptor binding. These two methods are simple but easily biased due to the blood-brain barrier transport compared to the 3- or 4-compartment model analysis,⁴¹ and they are also biased because of the change in cerebellar blood flow because the cerebellum was used as the standard region. The CBF effect on the rNMPB ratio must therefore be considered when we interpret the data obtained. The discrepancy between our results and those of Zubieta may be due to the differences between the analytical methods (rNMPB ratio vs. 3-compartment model analysis), although a decrease in mACh-R in the hypometabolic cerebral cortices in AD did seem to exist.

CONCLUSION

The results of our study suggest that mACh-R decreased in patients with AD, and that ^{18}F FDG PET was the most

sensitive method for detecting the degenerative regions in patients with AD.

ACKNOWLEDGMENTS

The authors thank Dr. Osamu Inoue of Osaka University and Dr. Kazutoshi Suzuki of the National Institute of Radiological Sciences for their pharmaceutical advice and we also thank Dr. Kouhei Akazawa of Department of Medical Informatic for statistical advice and Dr. Brian T. Quinn of Department of Literature for editorial assistance. This work was partly supported by Grant No. 6B-2 and a No. 94A-2401-4 from the Japanese Ministry of Health and Welfare, and a Grant-in-Aid (05670781) for Scientific Research from the Japanese Ministry of Education, Science and Culture.

REFERENCES

1. Bartus RT, Dean RL III, Beer B, Lippa AS. The cholinergic hypothesis of geriatric memory dysfunction. *Science* 217: 408–417, 1982.
2. Coyle JT, Price DL, Delong MR. Alzheimer's disease: a disorder of cortical cholinergic innervation. *Science* 219: 1184–1190, 1983.
3. Mash DC, Flynn DD, Potter, LT. Loss of M2 muscarinic receptors in the cerebral cortex in Alzheimer's disease and experimental cholinergic denervation. *Science* 228: 1115–1117, 1985.
4. Holman BL, Gibson RE, Hill TC, Eckelman WC, Albert M, Reba RC. Muscarinic acetylcholine receptors in Alzheimer's disease. *JAMA* 254: 3063–3066, 1985.
5. Lee KS, Frey KA, Koeppe RA, Buck A, Mulholland GK, Foster NL, et al. Quantification of muscarinic cholinergic receptors in aging and Alzheimer's disease. *J Nucl Med* 32: 942–943, 1991. (Abstract)
6. Mulholland GK, Kilbourn MR, Sherman P, Carey JE, Frey KA, Koeppe RA, et al. Synthesis, *in vivo* biodistribution and dosimetry of [^{11}C]N-methylpiperidyl benzilate ([^{11}C]NMPB), a muscarinic acetylcholine receptor antagonist. *Nucl Med Biol* 22: 13–17, 1995.
7. Mulholland GK, Jewett DM, Otto CA, Kilbourn MR, Sherman PS, Kuhl DE. Synthesis and regional brain distribution of [^{11}C]N-methyl-4-piperidyl benzilate ([^{11}C]NMPB) in the rat. *J Nucl Med* 29: 768, 1988. (Abstract)
8. Koeppe RA, Frey KA, Zubieta JA, Fessler JA, Mulholland GK, Kilbourn MR, et al. Tracer analysis of [^{11}C]N-methyl-4-piperidyl benzilate binding to muscarinic cholinergic receptors. *J Nucl Med* 33: 882, 1992. (Abstract)
9. Zubieta JK, Frey KA, Koeppe RA, Kilbourn MR, Mulholland GK, Foster NL, et al. Muscarinic receptor binding in aging and Alzheimer's disease determined with [C-11]N-methyl-4-piperidyl benzilate and PET. *J Nucl Med* 35: 20, 1994. (Abstract)
10. McKhann G, Drachman D, Folstein M, Katzman R, Price D, Stadlan EM. Clinical diagnosis of Alzheimer's disease: report of the NINCDS-ADRDA work group under the auspices of Department of Health and Human Services task force on Alzheimer's disease. *Neurology* 34: 939–944, 1987.
11. American Psychiatric Association. *Diagnostic and Statistical*

- cal Manual of Mental Disorders, revised 3rd eds (DSM-III-R). American Psychiatric Association, Washington, 1987.
12. Folstein MF, Folstein SE, McHugh PR. "Mini Mental State." A practical method for grading the cognitive state of patients for the clinician. *J Psychiatr Res* 12: 189-198, 1975.
13. Hasegawa K, Inoue K, Moriya K. An investigation of dementia rating scale for the elderly. *Seishinigaku* 16: 965-969, 1974. (in Japanese)
14. Suhara T, Inoue O, Kobayashi K, Suzuki K, Tateno Y. Age-related changes in human muscarinic acetylcholine receptors measured by positron emission tomography. *Neuroscience Letters* 149: 225-228, 1993.
15. Bida GT, Satyamurthy N, Barrio JR. The synthesis of 2-[F-18]-fluoro-2-deoxy-D glucose using glycals: a reexamination. *J Nucl Med* 25: 1327-1334, 1984.
16. Chang LT. Group Research. A method for attenuation correction in radionuclide computed tomography. *IEEE Transactions on Nuclear Science* NS-25: 638-643, 1978.
17. Lassen NA, Anderson AR, Friberg L, Paulson OB. The retention of [^{99m}Tc]-D,L-HMPAO in the human brain after intracarotid bolus injection: a kinetic analysis. *J Cereb Blood Flow Metabol* 8 (suppl 1): S13-S22, 1988.
18. Phelps ME, Huang SC, Hoffman EJ, Selin C, Sokoloff L, Kuhl DE. Tomographic measurements of local cerebral glucose metabolic rate in humans with [¹⁸F]2-fluoro-2-deoxy-D-glucose: Validation of method. *Ann Neurol* 6: 371-388, 1979.
19. Brooks RA. Alternative formula for glucose utilization using labeled deoxyglucose. *J Nucl Med* 23: 538-539, 1982.
20. Gjedde A. Calculation of cerebral glucose phosphorylation from brain uptake of glucose analogs *in vivo*: a reexamination. *Brain Res Rev* 4: 237-274, 1982.
21. Patlak CS, Blasberg RG, Fenstermacher JD. Graphical evaluation of blood-to-brain transfer constants from multiple-time uptake data. *J Cereb Blood Flow Metabol* 3: 1-7, 1983.
22. Wong DF, Wagner HN Jr, Dannals RF, Links JM, Frost JJ, Ravert HY, et al. Effects of age on dopamine and serotonin receptors measured by positron tomography in the living human brain. *Science* 226: 1393-1396, 1984.
23. Dawson-Saunders B, Trapp RG. *Basic and Clinical Biostatistics*, 1st ed. Prentice Hall, 1990.
24. Rosner B. *Fundamentals of Biostatistics*, 4th ed. Duxbury Press, 1995.
25. Nordberg A. Neuroreceptor changes in Alzheimer disease. *Cerebrovasc Brain Metab Rev* 4: 303-328, 1992.
26. Weinberger DR, Jones DW, Reba RC, Mann U, Coppola R, Gibson R, et al. A comparison of FDG PET and IQNB SPECT in normal subjects and in patients with dementia. *J Neuro-psychiatry Clinical Neurosci* 4: 239-248, 1992.
27. Wyper DJ, Brown D, Patterson J, Owens J, Hunter R, Teasdale E, et al. Deficits in iodine-labeled 3-quinuclidinyl benzilate binding in relation to cerebral blood flow in patients with Alzheimer's disease. *Eur J Nucl Med* 20: 379-386, 1993.
28. Caulfield MP, Stragham DW, Cross AJ, Crow T, Birdsall NJ. Cortical muscarinic subtypes and Alzheimer's disease. *Lancet* ii: 1277, 1982.
29. Lee KS, Frey KA, Koeppe RA, Buck A, Mulholland GK, Kuhl DE. *In vivo* quantification of cerebral muscarinic receptors in normal human aging using positron emission tomography and [¹¹C]tropanyl benzilate. *J Cereb Blood Flow Metabol* 16: 303-310, 1996.
30. Buck A, Mulholland GK, Papadopoulos SM, Koeppe RA, Frey KA. Kinetic evaluation of positron-emitting muscarinic receptor ligands employing direct intracarotid injection. *J Cereb Blood Flow Metabol* 16: 1280-1287, 1996.
31. Asahina M, Shinotoh H, Hirayama K, Suhara T, Shishido F, Inoue O, et al. Hypersensitivity of cortical muscarinic receptors in Parkinson's disease demonstrated by PET. *Acta Neurol Scand* 91: 437-443, 1995.
32. Fukuyama H, Ogawa M, Yamauchi H, Yamaguchi S, Kimura J, Yonekura Y, et al. Altered cerebral energy metabolism in Alzheimer's disease. *J Nucl Med* 35: 1-6, 1994.
33. Korf J, Gramsbergen JB. Hippocampus pathology in dementia: postmortem assessed cation shifts and amino acid transmitter contents and its possible neuroimaging *in vivo*. *Electroencephalogr Clin Neurophysiol* 42 (suppl): 366-379, 1991.
34. Ohnishi T, Hoshi H, Nagamachi S, Jinnouchi S, Flores LG II, Futami S, et al. High-resolution SPECT to assess hippocampal perfusion in neuropsychiatric diseases. *J Nucl Med* 36: 1163-1169, 1995.
35. Alavi A, Newberg AB, Souder E, Berlin JA. Quantitative analysis of PET and MRI data in normal aging and Alzheimer's disease: atrophy weighted total brain metabolism and absolute whole brain metabolism as reliable discriminators. *J Nucl Med* 34: 1681-1687, 1993.
36. Frackowiak RSJ, Pozzilli C, Legg NJ, Du Boulay GH, Marshall J, Lenzi GL, et al. Regional cerebral oxygen supply and utilization in dementia: a clinical and physiological study with oxygen-15 and positron tomography. *Brain* 104: 753-778, 1981.
37. Butler RW, Dickinson WA, Katholi C, Holsey JH. The comparative effect of organic brain disease on cerebral blood flow and measured intelligence. *Ann Neurol* 13: 155-159, 1983.
38. O'Brien JT, Eagger S, Syed GMS, Sahakian BJ, Levy R. A study of regional cerebral blood flow and cognitive performance in Alzheimer's disease. *J Neurol Neurosurg Psychiatry* 55: 1182-1187, 1992.
39. Wong DF, Gjedde A, Wagner HN Jr. Quantification of neuroreceptors in the living human brain. I. Irreversible binding of ligands. *J Cereb Blood Flow Metabol* 6: 137-146, 1986.
40. Lin SC, Olson KC, Okazaki H, Richelson E. Studies on muscarinic binding site in human brain identified with [³H]pirenzepine. *J Neurochem* 46: 247-279, 1986.
41. Koeppe RA, Frey KA, Mulholland GK, Kilbourn MR, Buck A, Lee KS, et al. [¹¹C]tropanyl benzilate-binding to muscarinic cholinergic receptors: methodology and kinetic models alternatives. *J Cereb Blood Flow Metabol* 14: 85-99, 1994.